

HEALTH AND MEDICINE

LiQD Cornea: Pro-regeneration collagen mimetics as patches and alternatives to corneal transplantation

Christopher D. McTiernan^{1,2,3*}, Fiona C. Simpson^{1,2*}, Michel Haagdoorens⁴, Chameen Samarawickrama^{5,6}, Damien Hunter⁵, Oleksiy Buznyk⁶, Per Fagerholm⁶, Monika K. Ljunggren⁶, Philip Lewis⁷, Isabel Pintelon⁸, David Olsen⁹, Elle Edin^{1,2}, Marc Groleau¹, Bruce D. Allan^{10†}, May Griffith^{1,2†}

Transplantation with donor corneas is the mainstay for treating corneal blindness, but a severe worldwide shortage necessitates the development of other treatment options. Corneal perforation from infection or inflammation is sealed with cyanoacrylate glue. However, the resulting cytotoxicity requires transplantation. LiQD Cornea is an alternative to conventional corneal transplantation and sealants. It is a cell-free, liquid hydrogel matrix for corneal regeneration, comprising short collagen-like peptides conjugated with polyethylene glycol and mixed with fibrinogen to promote adhesion within tissue defects. Gelation occurs spontaneously at body temperature within 5 min. Light exposure is not required—particularly advantageous because patients with corneal inflammation are typically photophobic. The self-assembling, fully defined, synthetic collagen analog is much less costly than human recombinant collagen and reduces the risk of immune rejection associated with xenogeneic materials. In situ gelation potentially allows for clinical application in outpatient clinics instead of operating theaters, maximizing practicality, and minimizing health care costs.

INTRODUCTION

The cornea is the transparent front surface of the eye that provides about two-thirds of the focusing power of the eye. Any permanent transparency loss from injury or disease can result in blindness. Currently, 23 million people globally have unilateral corneal blindness, while 4.9 million are bilaterally blind (1). Transplantation with human donor corneas has been the mainstay for treating corneal blindness for a century. However, a global donor cornea shortage leaves 12.7 million on waiting lists, with only 1 in 70 patients treated (2).

Conditions requiring corneal transplantation include persistent ulceration leading to scarring or perforation after corneal infection, burns, autoimmune diseases, and physical trauma. Corneal perforations are an emergency, and in many centers, the cornea is temporarily sealed using cyanoacrylate glue to maintain integrity and avoid losing the eye (3). However, cyanoacrylate glue is toxic and can cause local irritation and inflammation. Its incomplete polymerization leaves behind toxic cyanoacrylate monomers, while its hydrolysis releases potentially toxic compounds like formaldehyde and alkyl cyanoacrylate (4). These induce corneal scarring and vascularization. Patients generally require follow-up corneal transplantation. Despite these clear limitations, the use of cyanoacrylate glue to seal corneal perforations has remained the established emergency treatment for

more than 50 years (5). Other interventions include corneal suturing (6), tectonic corneal grafts (7), conjunctival flaps (8), multilayered amniotic membrane transplantation (9), soft “bandage” contact lenses (10), and tissue sealants.

Sealants examined include a variety of natural adhesives like fibrin, gelatin, chitosan, and alginate (11), as well as a number of synthetic polyethylene glycol (PEG) derivatives (12). Most of these interventions, however, work only in a limited range of cases or require invasive surgery with possible limitations for future visual rehabilitation (13).

PEG-based sealants have shown promise in sealing perforating microincisions, but to the best of our knowledge, there is no study which has looked at their efficacy in sealing macroperforations. Furthermore, PEG-based sealants typically require multicomponent mixing and suffer from short application windows. For example, ReSure (Ocular Therapeutix Inc.), which requires two-component mixing of PEG and a trilycine acetate solution, allows only a 20-s window for application upon initiation of polymerization (14).

A new bioadhesive, GelCORE, was recently reported as an alternative to cyanoacrylate glue for corneal tissue repair in partial-thickness corneal defects and corneal perforations. The authors used white light, with Eosin Y, triethanolamine (TEA), and *N*-vinylcaprolactam (VC) as initiators to gel a mixture of methacryloyl functionalized gelatin in situ (11). The GelCORE report included a 14-day rabbit study in which a 50% thickness wound was repaired. However, because of the short duration of the study, long-term effects could not be evaluated. The use of animal-derived gelatin has an associated risk of zoonotic disease transfer, and severe allergic reactions to both bovine and porcine gelatin in vaccines have been reported (15). Photocrosslinking may also be problematic in the clinical setting. Patients with corneal inflammation are photophobic (light-sensitive) and may not be able to tolerate intense visible light application more than 4 min without retrobulbar or general anesthesia. In a mechanism analogous to corneal cross-linking for keratoconus, the creation of free radicals in photocrosslinking may also be toxic to the corneal endothelium in thinned or perforated corneas (16). Hyaluronic

¹Centre de Recherche Hôpital Maisonneuve-Rosemont, Montréal, QC, Canada. ²Department of Ophthalmology and Institute of Biomedical Engineering, Université de Montréal, Montréal, QC, Canada. ³Division of Cardiac Surgery, University of Ottawa Heart Institute, Ottawa, ON, Canada. ⁴Department of Ophthalmology, Visual Optics and Visual Rehabilitation, University of Antwerp, Antwerp, Belgium. ⁵Centre for Vision Research, The Westmead Institute for Medical Research, and Faculty of Medicine and Health, University of Sydney, Sydney, Australia. ⁶Institute for Clinical and Experimental Medicine, Linköping University, Linköping, Sweden. ⁷School of Optometry and Vision Sciences, Cardiff University, Cardiff, UK. ⁸Laboratory of Cell Biology and Histology, University of Antwerp, Antwerp, Belgium. ⁹FibroGen Inc., San Francisco, CA, USA. ¹⁰NIHR Biomedical Research Centre at Moorfields Eye Hospital NHS Foundation Trust and UCL Institute of Ophthalmology, London, UK.

*These authors contributed equally to this work.

†Corresponding author. Email: may.griffith@umontreal.ca (M. Griffith); bruce.allan@ucl.ac.uk (B.D.A.)

acid-based materials have also been tested as alternative bioadhesives in an *in vitro* organ setting using excised porcine eyes (17). This solution relied on hydrazone cross-linking of dopamine-modified hyaluronic acid (HA-DOPA), where dopamine supplied the tissue adhesive properties. While successful *in vitro*, this material has not been evaluated in animal models. Neither GelCORE nor HA-DOPA was tested for repair of full-thickness corneal perforations, nor have they been examined as alternatives to donor corneal tissue for transplantation.

Over 10 years ago, our team members conducted a first-in-human clinical trial on cell-free, biosynthetic hydrogels made from recombinant human collagen type III (RHCIII). These hydrogels promoted stable corneal tissue and nerve regeneration, showing that they were immune-compatible alternatives to donor cornea transplantation in anterior lamellar keratoplasty (ALK) (18, 19). Recently, we demonstrated that hydrogel implants derived from a short collagen-like peptide (CLP) conjugated to an inert, but mechanically robust, multifunctional PEG are functionally equivalent to the RHCIII-based implants when tested under preclinical conditions in mini-pigs (20). The use of fully defined short synthetic peptides provides homogeneous materials that are easily modified and scaled up in comparison to their full-length analogs. In addition to being fully synthetic, the use of CLP-PEG collagen analogs circumvents the batch-to-batch heterogeneity seen with extracted proteins, as well as potential allergic reactions to xenogeneic proteins (21) and possible zoonotic disease transmission (22). Despite being able to promote regeneration, these solid implants require an operating theater for implantation, involving costs for a full surgical team. Realistically, to reach the enormous numbers of patients awaiting transplantation, most of them living in low to middle income countries, we need a drastic paradigm change.

To date, vaccines have been vastly successful both in cost and delivery, with every person receiving a vaccine delivered in a syringe. By analogy, in dentistry, when someone has a cavity in a tooth, the pathologic tissue is removed, and the tooth is filled. A similar paradigm is likely needed to tackle this important global issue, where the pathologic tissue is replaced by a regeneration-stimulating liquid corneal replacement, LiQD Cornea, in a syringe that gels *in situ*. Previously, we reported that CLP-PEG polymerizes *in situ* and can form a seal in experimental *in vitro* models of corneal perforation when supported by an *ab interno* patch (23). In this study, we introduce the LiQD Cornea, a new injectable hydrogel matrix with adhesive properties. We examined the potential efficacy of our LiQD Cornea comprising CLP-PEG-fibrinogen as a sealant/filler of full-thickness corneal perforations and an alternative to lamellar corneal transplantation that potentially allow treatments to be carried out in an ophthalmologist's office.

RESULTS

Physical and mechanical characterization

The CLP-PEG-fibrinogen LiQD Cornea formed a porous hydrogel upon gelation in the presence of thrombin and a nontoxic cross-linker, 4-(4,6-dimethoxy-1,3,5-triazin-2-yl)-4-methylmorpholinium chloride (DMTMM) (fig. S1). LiQD Cornea hydrogel samples showed a refractive index of 1.354 ± 0.037 , consistent with human corneas and physical and chemical properties consistent with previous generations of RHCIII and CLP-PEG hydrogels (Table 1) (18, 20). In the visible spectrum (400 to 800 nm), LiQD Cornea samples transmitted between 93 and 99% of incident light. The transmission

of light in the ultraviolet (UV) region decreased to a low value of 19% in the UV-C spectral region. Bursting pressure testing using *ex vivo* porcine corneas showed that the LiQD Cornea formulation, although less robust than cyanoacrylate or fibrin sealant, nevertheless withstood 170 mmHg of pressure. This was a 7.7-fold increase over the average 11 to 21 mmHg of intraocular pressure within the human eyeball (Table 1).

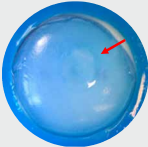
In vitro characterization

Human corneal epithelial cells (HCECs) from an immortalized line (24) adhered to and spread readily on *in vitro* gelled matrices, indicating that the LiQD Cornea supports epithelial growth (Fig. 1A). The materials were also found to be immune compatible. Precursors of murine bone marrow-derived macrophage (BMDM) cells seeded on LiQD Cornea hydrogels in the presence of macrophage differentiation media showed higher levels of expression of CD206 (anti-inflammatory M2 marker) in comparison to CD86 (pro-inflammatory M1 marker) at the time points examined (Fig. 1B). This showed a polarization of the mononuclear macrophage precursors into anti-inflammatory or tolerizing phenotypes. Exposure of bone marrow-derived dendritic cells (BMDCs) to the LiQD Cornea hydrogel and its components resulted in low expression of CD40, CD80, and CD86, which are markers of activated, antigen-presenting dendritic cells. This showed that overall, the LiQD Cornea formulation did not activate dendritic cells, which are the main cells associated with triggering graft rejection (25). By comparison, dendritic cells showed significant activation marker expression when exposed to the positive lipopolysaccharide (LPS) controls (Fig. 1C).

In vivo rabbit perforation study

In accordance with the Association for Research in Vision and Ophthalmology (ARVO) Statement for the Use of Animals in Ophthalmic and Visual Research and with ethical permission from the Western Sydney Local Health District Animal Ethics Committee (Australia), conical perforations were made in one cornea each in three New Zealand white rabbits. The perforations measured 3 mm in diameter on the external epithelial surface tapering to 1 mm on the internal endothelial surface. To seal the wound gape, we first applied thrombin solution to the wound margins. Then, a mixture of CLP-PEG-fibrinogen and DMTMM cross-linker was applied. As the gel sets, the thrombin that was applied to the wound surface converted the fibrinogen at the interface of the gel to fibrin, adhering the gel firmly to the wound. DMTMM then cross-links the entire mixture. The surgically created perforations were completely sealed with the LiQD Cornea hydrogel, as indicated by the retention of an air bubble placed within the anterior chamber (Fig. 1E). Two rabbits had a complete seal with the first application, while the third cornea required additional material for an air-tight seal. All animals received antibiotic (chloramphenicol) and anti-inflammatory (dexamethasone) eye drops three times daily for 3 days. There was no incidence of leakage or infection of the perforation sites in any animal, and by 7 days after surgery, all normal peri-surgical inflammation had subsided. The hydrogels initially showed haze that began to recede 1 day after surgery. At 28 days follow-up, two of three rabbits had transparent corneas (Fig. 1E) and normal slit lamp exams. In the third rabbit, the gel remained visible as a slight haze in the cornea. Histopathology of the cornea showed epithelial hyperplasia and reduced corneal stroma in the perforation site, indicating that the perforation site of each cornea had undergone reepithelialization.

Table 1. Optical, physical, and mechanical properties of LiQD Cornea hydrogels.

| Tensile strength (MPa) | Modulus (MPa) | Viscosity (Pa.s) | Transmission (%) | Refractive index | Water content (%) | Collagenase (mg/min) | T_d (°C) |
|------------------------|-----------------------------------|------------------|---------------------------------|---|-------------------|---|------------|
| 0.02 | 0.16 | 31.7 ± 27.6 | 19–93% (UV) 93–99% (Visible) | 1.354 ± 0.037 | 91.2 ± 2.3 | $7.3 \times 10^{-7} \pm 6.1 \times 10^{-7}$ | 64 ± 8.5 |
| Material | Average bursting pressure (mmHg)* | | | Representative image of sealed ex vivo perforation model† | | | |
| Cyanoacrylate glue | >300 | | |  | | | |
| Fibrin sealant | 259 ± 14.5 | | |  | | | |
| LiQD Cornea | 170 ± 16.9 | | |  | | | |

*Maximum pressure measured by the pressure transducer is 300 mmHg. †Photographs of ex vivo porcine corneas, which were mounted in an artificial anterior chamber and perforated according to the described model and sealed/filled with the corresponding material. Red arrows highlight the interface of the applied material and the perforated cornea.

There was also keratocyte infiltration, indicating the onset of corneal stromal regeneration, and partial regeneration of Descemet's membrane. Furthermore, when LiQD Cornea was applied to the perforated corneas of the rabbits, the gel remained cohesive with itself and generally did not leak into the anterior chamber. While there was small degree of postoperative anterior chamber inflammation on day 1, this subsided by day 3 and remained that way for the duration of the study.

In vivo study in Göttingen mini-pigs

Genetically uniform Göttingen mini-pigs were used (26) in compliance with the Swedish Animal Welfare Ordinance and the Animal Welfare Act and with ethical permission from the local ethical committee (Linköpings Djurförsöksetiska Nämnd). Anterior lamellar keratoplasty wound beds, 6.5 mm in diameter, 500 μ m deep (i.e., over 70% depth), were made in one cornea each of four mini-pigs by trephination, followed by dissection with a blade. LiQD Cornea was applied as for the rabbits. Figure S2A shows the progress of repair and regeneration of all pigs receiving the LiQD Cornea compared to syngeneic grafts and healthy unoperated controls. At 12 months, the application of LiQD Cornea was successful in all pigs (Fig. 1F), although in all cases, the surgeon applied the LiQD Cornea at least twice, removing the first material before reapplication to achieve the desired curvature. One pig, which received four attempts at LiQD Cornea application, underwent full corneal perforation and was given a suture to bridge the unintended gape. Postsurgical optical coherence tomography (OCT) of the LiQD Cornea application (fig. S2B) showed

that although the initial LiQD Cornea fills were imperfect, the anterior corneal surfaces of all four pigs were smooth and followed the contours of the host tissue by 3 months after operation. These results also show that an easy-to-use point-of-care (POC) delivery device (fig. S3) is merited for future clinical application.

Clinical follow-up showed that at 1-month follow-up, all pigs had successfully reepithelialized. At 3 months after surgery, pachymetric analyses showed that the standard corneal thickness was restored in LiQD Cornea animals (Fig. 3A and fig. S2B). Intraocular pressure was normal at all postsurgical exams, indicating that the LiQD Cornea successfully sealed the surgical site (Fig. 2B). The LiQD Cornea pigs showed more significant haze and neovascularization than syngeneic grafts at all postsurgical time points, but haze was reduced in three of four animals at 12 months after operation (Fig. 2, C and D). The fourth pig had poor surgical results with iritis and formation of peripheral anterior synechiae (attachment of the iris to the cornea) and infiltration of a large blood vessel into the surgical site, resulting in a hazy cornea at 12 months after operation. This pig had inadvertently received a full-thickness corneal perforation that was reattached with a suture that trekked in a large blood vessel. This pig, nevertheless, showed full regeneration of corneal tissue and nerves. Esthesiometry performed to determine touch sensitivity showed the restoration of the corneal blink response in all operated corneas, indicating the presence of regenerated nerves within the graft site (Fig. 2E). Analysis of the density of corneal nerves over time showed that by 12 months after operation, there were no statistically significant differences in the nerve density (Fig. 2F) between the LiQD

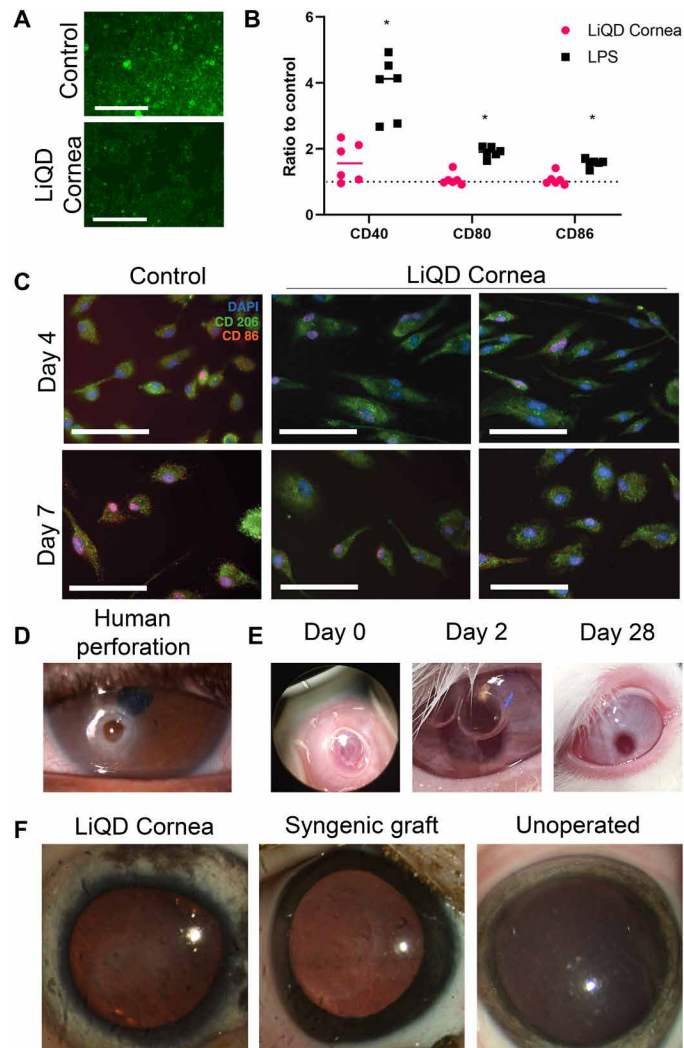


Fig. 1. Biological evaluation of LiQD Cornea. (A) Immortalized HCECs cultured on LiQD Cornea hydrogels and control tissue culture plastic, showing that the hydrogels support epithelial growth. (B) Expression of T cell costimulatory molecules in BMDCs. Expression of CD40, CD80, and CD86 was measured by flow cytometry, and data are presented as a ratio of mean fluorescence intensity of the experimental samples to untreated BMDCs. LPS acted as a positive control for BMDC activation; * $P \leq 0.05$ by Student's *t* test. (C) Expression of pro-inflammatory M1 (CD86) and anti-inflammatory M2 (CD206) phenotypic markers at 4 and 7 days after exposure of naïve BMDM precursors to LiQD Cornea hydrogels. (D) Example of a human corneal perforation. (E) Postsurgical photos of rabbits immediately after injecting LiQD Cornea into a perforated cornea. The two-stepped surgically induced perforation can be seen. At day 2 after surgery, the air bubble placed under the cornea during surgery is prominent, indicating that the perforation was completely sealed. The perforated cornea was completely healed by 28 days after operation. Photo credit: Damien Hunter, University of Sydney. (F) Mini-pig corneas where the LiQD Cornea was tested as an alternative to a donor allograft, showing the gross appearance of the LiQD Cornea, syngeneic graft, and an unoperated eye at 12 months after surgery. Photo credit: Monika K. Ljunggren, Linköping University.

Cornea ($3012.8 \pm 1613.7 \mu\text{m}^2$), syngeneic ($2205.3 \pm 1162.4 \mu\text{m}^2$), and unoperated control ($4800.4 \pm 1964.9 \mu\text{m}^2$). However, it is clear that the unoperated controls had a higher nerve density. There were no marked differences in tear production in the three treatment groups at any time point, as indicated by Schirmer's test (Fig. 2G).

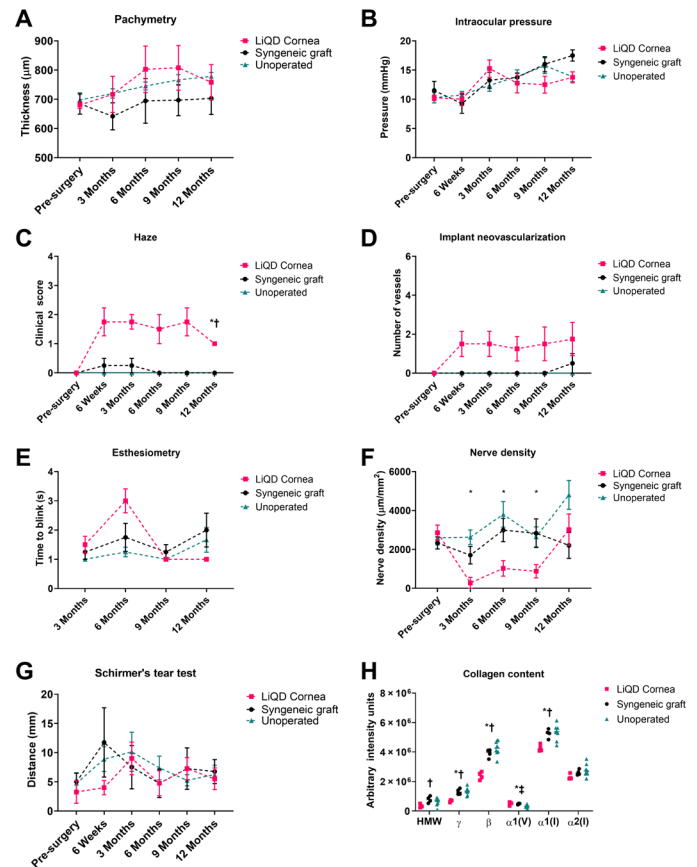


Fig. 2. Clinical exam progression of LiQD Cornea in Göttingen mini-pigs. (A) Pachymetry showing corneal thickness measured by OCT, showing no significant differences in thickness compared to controls. There was a normal increase in corneal thickness in unoperated controls as the pigs matured. (B) Intraocular pressures were similar in all three groups, showing a slight overall increase over the normal aging process of the pigs. (C) Central corneal haze measured using a modified McDonald-Shadduck scoring system on a scale from 0 to 4. An increase of haze corresponds to the period of in-growth of stromal cells into the cell-free implants. By 12 months after operation, the cells appeared to have attained quiescence. (D) Corneal neovascularization was seen in the LiQD Cornea, mainly from the animal that sustained an unintended perforation. (E) Corneal blink response measured by Cochet-Bonnet esthesiometry showed no significant differences among the three groups. (F) Corneal nerve density in the LiQD Cornea group was significantly lower than the unoperated corneas during months 3 to 9 after operation when the severed nerves were regenerating. (G) Schirmer's tear test showed similar responses in all three groups tested. (H) Expression of high-molecular weight collagens (HMW, γ , and β), type V collagen, and type I collagen ($\alpha 1$ and $\alpha 2$) in the central portion of the cornea. Figures (A), (B), and (E) to (H) were assessed using a mixed-effects model with a Tukey post hoc test for multiple comparisons. Figures (C) to (D) were analyzed using a Mann-Whitney *U* test for ordinal data. * $P \leq 0.05$ for LiQD Cornea to unoperated, † $P \leq 0.05$ for LiQD Cornea to syngeneic graft, and ‡ $P \leq 0.05$ syngeneic graft to unoperated. All data are plotted as mean \pm SEM or mean with individual values.

Collagen content analysis of the central cornea demonstrated significantly lower levels of high-molecular weight, γ -, β -, $\alpha 1(V)$ -, and $\alpha 1(I)$ -type collagen in the LiQD Cornea pigs, as compared to the syngeneic grafts and unoperated eyes (Fig. 2H and table S5).

Hematoxylin and eosin sections of mini-pig corneas at 12 months after surgery showed that LiQD Cornea-treated corneas had regenerated their epithelia and stroma (Fig. 3A) and resembled

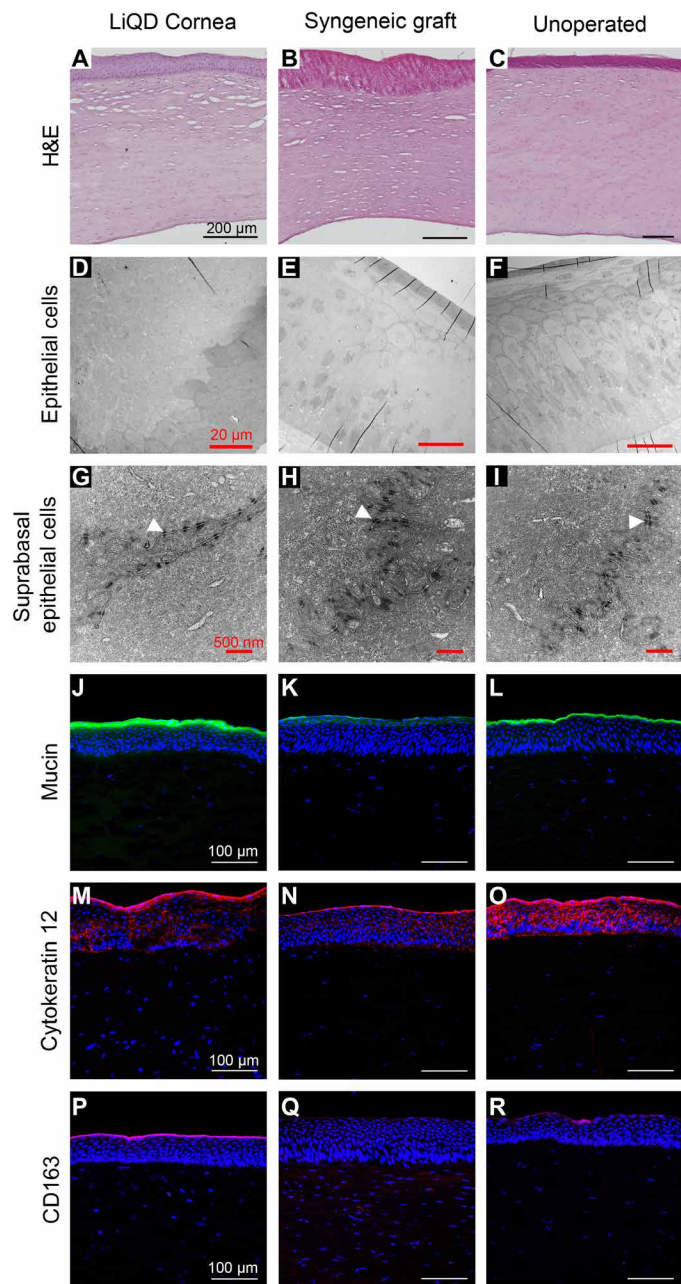


Fig. 3. Histopathology, TEM, and immunohistochemistry of the LiQD Cornea at 12 months. (A to C) Paraffin-embedded sections of porcine cornea stained with hematoxylin and eosin (H&E) show multilayered, nonkeratinizing epithelia in all three samples. (D to F) TEM images of corneal epithelium in all three samples. (G to I) Epithelial cells showed abundance of desmosomes between cells (arrowheads). (J to L) Fully regenerated corneal tear film mucin stained with fluorescein isothiocyanate-conjugated lectin (green) from *Ulex europaeus* is seen in the LiQD Cornea. This is similar to the tear film in the controls. (M to O) Cytokeratin 12 (red), a marker for fully differentiated corneal epithelial cells, is present in the regenerated LiQD Cornea as in controls. (P to R) CD163 staining (red) shows that a few mononuclear cells are present in stroma of all three samples. Cell nuclei were stained blue with DAPI.

corneas in the syngeneic graft (Fig. 3B) and untreated control groups (Fig. 3C). The unoperated endothelia remained healthy. Transmission electron microscopy (TEM) confirmed the presence of healthy electron-lucent epithelial cells in all three samples (Fig. 3, D to F).

There were no cells with condensed cytoplasm or pyknotic, shrunken nuclei that are characteristic of apoptotic cells. TEM also revealed that the basal epithelial cells in all samples had desmosomes between them (Fig. 3, G to I), showing that regenerated cells in the LiQD Cornea had tight junctions and were functional as a barrier. Immunohistochemical analysis showed the presence of mucin, indicating a functional tear film in all samples (Fig. 3, J to L), and epithelial cytokeratin 12, indicating terminal differentiation of regenerated epithelium (Fig. 3, M to O). All samples contained very few CD163⁺ cells from the monocyte/macrophage lineage (Fig. 3, P to R). Immunohistochemical staining for α -smooth muscle actin (α -SMA) (fig. S4, A to C) and the lymph vessel marker, lymphatic vessel endothelial hyaluronan receptor 1 (LYVE1) (fig. S4, D to F), respectively, showed no increase in staining for myofibroblasts or lymphatics in the LiQD Cornea, as compared to allografts.

TEM images of the epithelial-stromal junction show the presence of small vesicles in the epithelial cells in all three samples (Fig. 4, A to C). Immunohistochemical staining showed the presence of large numbers of Tsg101⁺ vesicles in the epithelium and stroma of LiQD Cornea-treated samples (Fig. 4D). Tsg101 is an established marker for extracellular vesicles (EVs), forming part of the endosomal sorting complex required for transport-I (ESCRT-I), which is necessary for exosome-dependent intercellular signaling and vesicular trafficking (27). The staining is more diffuse in the syngeneic grafts (Fig. 4E) and minimal in the untreated controls (Fig. 4F). The samples were also stained for the tetraspanin, CD9, another established EV marker that more specifically marks exosomes (28). Colocalization of Tsg101 with CD9 showed that exosomes were present in the basal epithelium and upper stroma in the LiQD Cornea pigs (Fig. 4G), to a lesser extent in syngeneic grafts (Fig. 4H) and only minimally in the untreated corneas (Fig. 4I).

In vivo confocal microscopy showed that the epithelium in the LiQD Cornea was fully regenerated at the 3-month examination time point and remained stable at the 12-month end point (Fig. 5A), resembling that of the syngeneic (Fig. 5B) and untreated corneas (Fig. 5C). Regenerated nerves were found within the sub-basal epithelium of the LiQD Cornea starting at 3 to 6 months after surgery. At 12 months after operation, the nerves present were in distinct parallel bundles (Fig. 5D), characteristic of the subepithelial nerve plexus, similar to those found in the healthy unoperated control corneas (Fig. 5F). Nerves in the syngeneic grafts were not as well defined in their configuration (Fig. 5E). From 3 to 9 months, reflective keratocytes indicative of in-growing cells were seen within the matrix. The presence of reflective cells corresponded with the increased haze seen by slit lamp biomicroscopy (Fig. 2C). At 12 months, keratocytes grew into the cell-free matrix to reconstitute the stroma (Fig. 5G). Most of these keratocytes were not reflective and resemble keratocytes in the syngeneic grafts (Fig. 5H) and untreated controls (Fig. 5I). The decrease in reflectivity likely corresponds to the decrease in haze in Fig. 2C.

DISCUSSION

To address the severe shortfall of donor tissue in the treatment of corneal blindness, it is imperative that novel alternatives to corneal transplantation and perforation repair are developed. While a number of techniques and materials are currently available to treat corneal defects and perforations, many of them involve complex procedures and use materials with poor biocompatibility, mechanical mismatch,

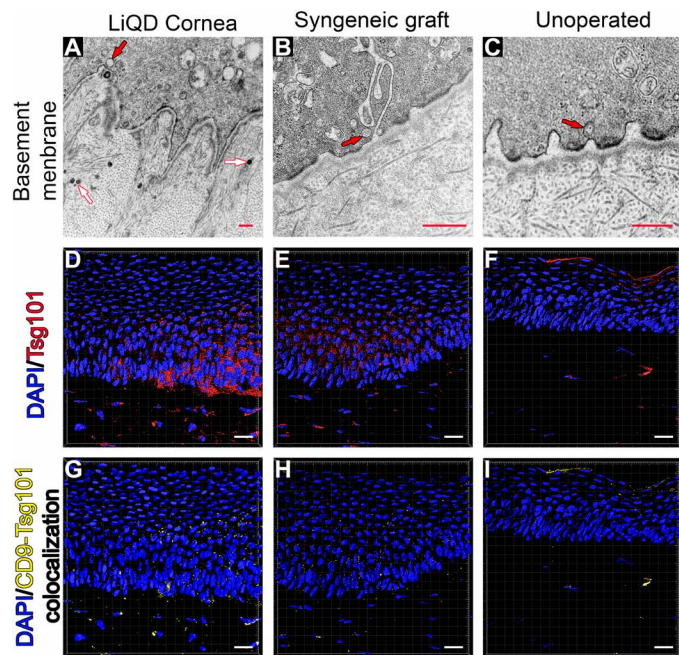


Fig. 4. EV and exosome secretion of the regenerated LiQD Cornea compared to a healthy unoperated cornea and a syngeneic graft. (A) Transmission electron micrograph of a LiQD Cornea sample showing the presence of basal epithelial cells invaginations into the stroma. A basement membrane was present. Vesicles can be seen inside the epithelial cell (an example is indicated with a red arrow). EVs are seen (white arrows) in the underlying stromal compartment. (B and C) TEM of syngeneic graft and unoperated cornea, respectively. (D to F) Surface reconstructions of corneal sections stained with the cytosolic, EV marker Tsg101 (red) and DAPI (blue). (G to I) Surface reconstruction of colocalized CD9 and Tsg101 staining indicating the presence of exosomes in the basal epithelium and upper stroma of the LiQD Cornea sample. There was less staining in the syngeneic graft and minimal in the untreated control. Scale bars: 500 nm (red) and 20 μ m (white).

and an inability to support regeneration. Ideally, any newly developed method should be easy to apply in a clinical setting, readily fill corneal defects, and seal perforations. At the same time, it should support tissue regeneration, limiting the need for further surgical intervention and follow-up corneal transplantation.

Our results showed that LiQD Cornea behaved as an injectable liquid at temperatures above 37°C, gelling as it cools down. In situ gelation of the LiQD Cornea in animal corneas took 5 min at body temperature, after initiation with DMTMM, a nontoxic cross-linker (23). Most patients with corneal perforations have inflamed eyes and are photophobic. Unlike light-activated systems, LiQD Cornea did not require a dedicated light source for curing. Without the requirement for light activation, no anesthetic will be needed in future clinical application to render the exposure to an intense light source for cross-linking tolerable. In addition, photoinitiated cross-linking has been reported to have possible phototoxic effects on the corneal endothelial cells (16). Considering that the initial perforation in pathologic corneas would also affect the health of the endothelium, it would be prudent not to further deplete the local population of endothelial cells.

The incorporation of an approved surgical fibrin sealant permitted adhesion of the LiQD Cornea during in situ gelation. Corneal perforations in ex vivo corneas were completely sealed in situ with a bursting pressure of 170 mmHg, which is several-fold higher than

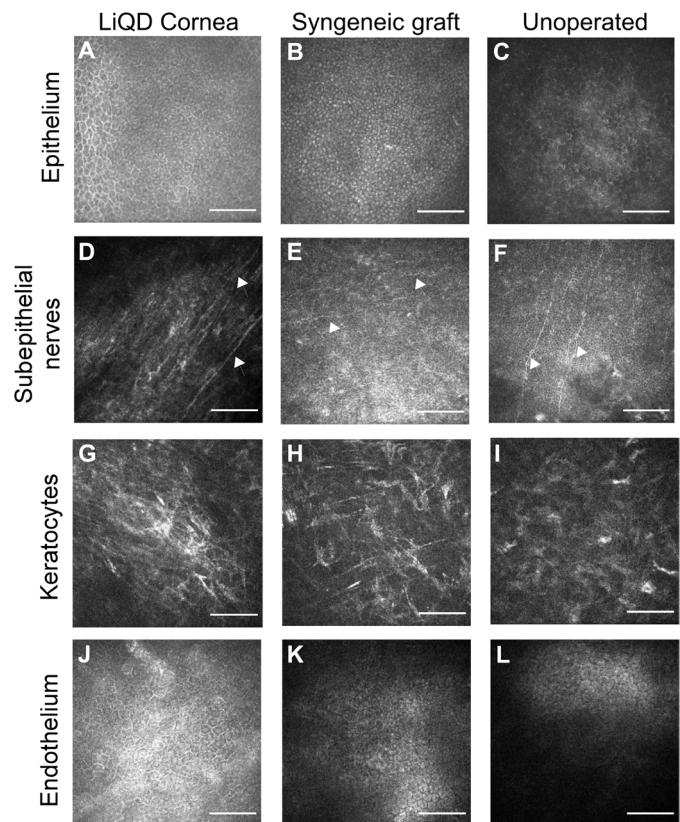


Fig. 5. In vivo confocal microscopy images of the LiQD Cornea compared to a healthy unoperated cornea and a syngeneic graft at 12 months after surgery. Regenerated corneal epithelial cells cover the surface of the LiQD Cornea (A) as with the syngeneic graft (B) and unoperated cornea (C). Regenerated nerves (arrowheads) were found at the sub-basal epithelium within the LiQD Cornea (D), ran parallel to one another, and were morphologically similar to those found in the unoperated cornea (F). Nerves in the syngeneic graft were less distinct (E). Keratocytes were present in all corneas (G to I). The unoperated endothelium remained intact and healthy in all corneas (J to L). Scale bars: 100 μ m.

normal intraocular pressures of 11 to 21 mmHg (29). HCECs grew readily on the LiQD Cornea hydrogels. The BMDC study indicated that the LiQD Cornea did not activate dendritic cells unlike the positive control, LPS, which is a well-established activator of dendritic cells. As the LiQD Cornea formulation does not activate dendritic cells, the risk of graft rejection due to activation of CD4⁺ and CD8⁺ T cells is reduced (30). The BMDM assay indicated that naïve BMDMs cultured in the presence of LiQD Cornea hydrogels primarily matured into an M2 phenotype that is associated with tolerogenic activity (31). These results taken together demonstrated that the LiQD Cornea formed a seal that will withstand the pressures encountered within the eye and will be fully biocompatible and immune compatible.

Injection of the LiQD Cornea into full-thickness corneal perforations in rabbits confirmed the ability to seal the wound gap. The completeness of the seal was validated by the addition of a postsurgical air bubble. The bubble was present up to 2 days after surgery, indicating that the material had created a complete seal that did not allow the leakage of air. The rabbit histology showed that the patch was completely reepithelialized. However, the 28-day duration of the study did not provide time for full stromal, endothelium, and nerve regeneration.

The Göttingen mini-pigs used were genetically coherent or homogenous. Hence, grafts from one animal to another were considered syngeneic, i.e., they were sufficiently identical and immunologically compatible to allow for transplantation. The 12-month *in vivo* pig study confirmed that LiQD Cornea allowed regeneration of the corneal epithelium, stroma, and nerves. Even if the material does not achieve the desired perfectly smooth surface directly after application, OCT results showed that the corneal thickness and curvature were restored to those matching the syngeneic grafts and unoperated controls (fig. S2B). The primary difference in the clinical performance of the LiQD Cornea and the syngeneic grafts was increased haze in the surgical site between 3 to 6 months after operation, during the period of rapid keratocyte in-growth into the cell-free matrix. Syngeneic grafts were already populated with donor cells, so no rapid in-growth of host cells was expected. However, at 1 year after surgery, the haze was reduced to a low grade in three of four LiQD Cornea recipients, while the syngeneic graft outline was still visible in the corneas. Neovascularization had accompanied the haze, as we had previously reported for solid CLP-PEG implants during the rapid cell population of cell-free grafts (20). However, as observed in previous solid implant studies (32, 33), the vessels receded over the 12-month observation period as haze cleared in three of four animals. While this small amount of vascularization and haze is not ideal, it is unlikely to lead to immune rejection. LiQD Cornea does not activate dendritic cells *in vitro* and is acellular and repopulated by the host cells, unlike traditional corneal transplants that bring with them allogeneic cells (25) whose surface proteins can trigger immune reactions. Vascularization could increase the risk of rejection of subsequent allografts (34), but LiQD Cornea is designed to regenerate the eye wall without the need for subsequent transplantation, avoiding problems with induced irregular astigmatism, rejection, and lack of access to transplant donor material. Where corneal perforations involve the central visual axis, at minimum, LiQD Cornea aims to restore eye wall integrity as a viable pathway for future rehabilitation. In our pig model, steroid medication was only administered for 5 days. In a clinical setting, it may be possible to modulate neovascularization during healing through application of topical steroids for a longer period.

We also found that LiQD corneas had lower expression of mature type I collagen in the cornea. This is in keeping with the fact that the LiQD Cornea matrix had no collagen, and hence, all collagen found at 12 months after surgery was due to active remodeling of the gel, in comparison to syngeneic grafts, which had a complete extracellular matrix at the time of grafting. When considering the relative performance of the LiQD Cornea and the syngeneic grafts, it is important to note that the syngeneic grafts are likely less inflammatory than a standard clinical allograft, because of the genetic homogeneity of Göttingen mini-pigs. As previously reported for CLP-PEG (20), the LiQD Cornea also induced the production of copious amounts of EVs that included exosomes, in comparison to the syngeneic grafts, and the lack of EVs in the untreated, healthy controls. We currently hypothesize that the presence of the EVs is linked to the production of new extracellular matrix in the surgical site, as the reduced collagen content in the LiQD Cornea suggests that the new tissue is still undergoing extracellular matrix protein secretion to restore the matrix at 12 months.

Overall, LiQD Cornea performed equivalently to syngeneic grafts, indicating a possible role as an alternative to conventional donor corneal transplantation for conditions treatable by lamellar trans-

plantation. However, as noted, it took the surgeon an average of two attempts to achieve the desired curvature, indicating that an appropriate point-of-care delivery device (fig. S3) is needed for clinical application. The self-assembling, fully defined, synthetic collagen-like LiQD Cornea is considerably less costly than human recombinant collagen and reduces any risk of allergy or immune rejection associated with xenogeneic materials. *In situ* gelation potentially allows for clinical application in an outpatient clinic instead of an operating theater, thereby maximizing practicality while minimizing health care costs.

MATERIALS AND METHODS

Synthesis of eight-arm CLP-PEG

The synthesis and characterization of CLP-PEG through conjugation of eight-arm PEG-maleimide to the 38 amino acid CLP via the formation of a thioether linkage has been previously described (23, 35). Successful conjugation of the CLP to the PEG-maleimide was confirmed through the disappearance of the vinylic proton peak at δ 7 parts per million by ^1H nuclear magnetic resonance spectroscopy and the appearance of characteristic vibrations in the Fourier transform infrared (FTIR) spectrum.

Here, CLP [CG(PKG)₄(POG)₄(DOG)₄] (AmbioPharm, SC, USA) was conjugated to a 40-K eight-arm PEG-maleimide with hexaglycerol core (Sinopeg Biotech Co Ltd., Beijing, China) to give rise to CLP-PEG (35). Briefly, 20 ml of water was degassed by sparging with N₂ for 20 min. The flask was charged with 770 mg of eight-arm PEG-maleimide, and the solution was stirred until complete dissolution was achieved. CLP (625 mg) was added to the stirring solution (molar ratio of eight-arm PEG-maleimide:CLP is 1:8). The solution was allowed to stir for an additional 20 min (at this point, all materials should be dissolved). The pH of the solution was adjusted to 4.5 through dropwise addition of 2 M NaOH. As the pH of the solution is adjusted, the reaction mixture becomes too viscous to be appropriately stirred. At this point, another 30 ml of N₂-purged water was added. The reaction flask was covered in aluminum foil and allowed to stir for 5 days. The pH of the reaction mixture was monitored periodically during this time and adjusted accordingly. At the end of the 5 days, an additional 50 ml of water was added to the reaction mixture, and again, the pH was adjusted to 4.5. The solution was filtered through a 0.45- μm syringe filter. The filtered solution was transferred to dialysis tubing (molecular weight cutoff: 14,000). The tubes were dialyzed against water (pH 4.5) for 7 days while exchanging the water every 12 hours. The contents of the dialysis bags were transferred to 50-ml Falcon tubes as 25-ml aliquots. The solutions were frozen overnight at -80°C and freeze-dried, resulting in a cotton-like solid CLP-PEG conjugate.

Reconstitution of CLP-PEG and fibrinogen at 10 and 1% (w/w), respectively

The plunger of a 10-ml sterile syringe with luer lock was removed, and the end was fitted with a syringe cap. CLP-PEG and fibrinogen (clottable protein, Tisseel, Baxter International, Deerfield, IL, USA) were added to the barrel of the syringe. HyPure molecular biology-grade water (GE Life Sciences, Logan, UT) was added to give a final dilution of 10 and 1% (w/w) for the CLP-PEG and fibrinogen, respectively. The syringe was then sealed with parafilm, and the CLP-PEG and fibrinogen was allowed to reconstitute at room temperature (RT) for 2 to 3 weeks. To facilitate the reconstitution process, the mixture was stirred periodically with a spatula and warmed up to 37°C in an

incubator. Once completely resuspended, the solution was heated above its melting temperature ($>37^{\circ}\text{C}$) and centrifuged at 3000 rpm for 10 min. This process was repeated until all bubbles had been removed from the syringe.

Reconstitution of thrombin

Thrombin was reconstituted at 250 U/ml by the addition of 4 ml of 10 mM phosphate-buffered saline (PBS) to the vial of thrombin contained within the Tisseel kit. The solution was mixed at RT for 20 min before use. The solution was either immediately used or aliquoted into several Eppendorf tubes and frozen at -20°C for future use. Frozen samples were thawed to RT before use.

Mixing and application of LiQD Cornea

The solution within the syringe containing 10% (w/w) CLP-PEG and 1% (w/w) fibrinogen behaves as a liquid (injectable) at temperatures above 37°C but sets as a gel when cooled to 25°C due to the templated assembly of the CLPs. However, this sol-gel transition is reversible. To make this sol-gel transition irreversible to obtain a hydrogel, a solution of the cross-linker DMTMM in 10 mM PBS was added to the mixture to obtain a final 2% (w/w) concentration of DMTMM while cooling down the solution of CLP-PEG and fibrinogen from 50° to 25°C .

For application into the cornea, the stock solution of CLP-PEG/fibrinogen was heated to 50°C and transferred to a 2-ml glass syringe and assembled within a T-piece mixing system that had been primed with 10 mM PBS. The T-piece system was heated to 50°C and mixed until homogeneous. A 10% (w/w) solution of DMTMM in 10 mM PBS was introduced through the injection port of the mixing system to give a final concentration of 2% (w/w) DMTMM. The solution was mixed within the T-piece system until homogeneous and then dispensed into the wound bed to which the solution of thrombin (250 U/ml) had been applied.

Physical and mechanical characterization

(i) Collagenase degradation assay

Collagenase from *Clostridium histolyticum* (Sigma-Aldrich) at 5 U/ml in 0.1 M tris-HCl buffer containing 5 mM CaCl_2 was used to evaluate the stability of the hydrogels as previously described. Briefly, samples were weighed after blotting off surface water at different time points to determine the rate of loss of mass. The percentage of residual weight was calculated using the following equation: Residual mass % = W_t/W_0 %, where W_t is the weight of hydrogel at a certain time point and W_0 is the initial weight of the hydrogel.

(ii) FTIR spectroscopy

Hydrogels were dried under vacuum for 3 days and measured using a Nicolet iS5 FTIR spectrometer equipped with an iD7 attenuated total reflectance sampling accessory with 4 cm^{-1} resolution; a total of 300 individual spectra were collected for each sample.

(iii) Differential scanning calorimetry

Denaturation temperature of the hydrogels was measured using a Q2000 differential scanning calorimetry (TA Instruments, New Castle, DE, USA). Heating scans were recorded in the range of 8° to 210°C at a scan rate of $10^{\circ}\text{C}/\text{min}$. Glass transition temperature (T_g) was measured as the onset of the endothermic peak.

(iv) Refractive index

The refractive index of the hydrogels was measured at RT on an Abbat 300 (Anton Paar) refractometer.

(v) Young's modulus and tensile strength

The Young's modulus and tensile strength of a $500\text{ }\mu\text{m}$ sheet of cross-linked material was evaluated in an Instron electromechanical universal tester (model 3342, Instron, Norwood, MA) equipped with Series IX/S software using a crosshead speed of 10 mm/min. The hydrogel was equilibrated in $1\times$ PBS for 1 hour before being cut into a 10 mm-by-5 mm rectangular piece. To remove surface water, the hydrogel was gently blotted with paper immediately before Instron measurement.

(vi) Water content of hydrogels

The water content of hydrogels was evaluated by weighing the "wet weight" (W_0) of the samples and then comparing this to the weight of the material after being dried at RT until a constant weight was achieved (W). The total water content of the hydrogels (W_t) was calculated according to the equation: $W_t\% = (W - W_0)/W\%$.

(vii) Pore size of hydrogels

Pore size measurements were made from scanning electron microscopy images obtained using a low-temperature scanning electron microscope in a Tescan (model: Vega II-XMU) with cold-stage sample holder at -50°C .

(viii) Viscosity of hydrogels

The viscosity of $500\text{-}\mu\text{m}$ hydrogels was measured on a Brookfield RS-CPS+ Rheometer (Brookfield Engineering Laboratories Inc., Middleboro, MA). The measurements were carried out at 37°C under parallel-plate geometry.

(ix) Light transmission of hydrogels

The light transmission of hydrogels between 250 and 800 nm was evaluated by placing a 5 mm-by-10 mm strip of hydrogel on the inside wall of a quartz cuvette filled with PBS and reading its absorption in a SpectraMax M2e series plate/cuvette spectrophotometer (Molecular Devices, San Jose, CA, USA). A cuvette filled with only PBS was used as the baseline reference. Measured absorbances were then converted to corresponding % transmission values.

Ex vivo model of corneal perforation and sealing evaluation

Corneoscleral buttons were excised from porcine eyes obtained from a local abattoir (Tom Henderson's Meats and Abattoir Inc., Chesterville, ON, Canada). The corneoscleral buttons were mounted on an artificial anterior chamber (Barron Artificial Anterior Chamber, Katena, NJ), and standardized corneal defects were made. Briefly, a 4-mm punch was used to partially trephine test corneas centrally to a depth of approximately $200\text{ }\mu\text{m}$. Lamellar dissection of the cap was performed with a pediatric crescent blade, leaving a residual stromal depth that was then trephined with a 3-mm punch to a depth of $200\text{ }\mu\text{m}$. A subsequent central full-thickness defect was created in the central stromal bed with a 1-mm skin biopsy punch to mimic a full-thickness corneal perforation commonly encountered in clinical practice.

(i) Sealing methods

Once the standardized corneal perforations had been made, one of three different materials was used to seal the defect. Each condition was repeated four times. Cyanoacrylate glue was injected to completely fill the defect. After allowing the glue to dry, the infusion was increased, and the bursting pressures were measured. For fibrin glue evaluation, fibrinogen (2%, w/w) and thrombin (250 U/ml) solutions were mixed (4:1) and transferred to completely fill the defect. After allowing the glue to dry, the infusion was increased, and the bursting pressures were measured. For the LiQD Cornea, the defect was coated with thrombin (250 U/ml). The LiQD Cornea was

injected to completely fill the defect. After allowing the glue to dry, the infusion was increased, and the bursting pressures were measured.

(ii) Bursting pressure evaluation

Artificial anterior chambers were connected via an intra-arterial blood pressure monitor (TruWave, Edwards Lifesciences) to a saline infusion bag using a pressure cuff to regulate infusion pressure. After application of test material, the infusion pressure was increased until the seal gave way, resulting in fluid egress. Bursting pressure (mmHg) was recorded as the peak in a continuous trace of infusion pressure versus time.

In vitro evaluation of the LiQD Cornea

The in vitro compatibility of the LiQD Cornea was tested using green fluorescence protein (GFP)-transfected immortalized HCECs (24). Briefly, three wells of a 24-well plate were coated with the LiQD Cornea. The glue was allowed to set for 1 hour before it was washed three times with 1 ml of 1× PBS. GFP-HCECs were seeded into the control wells and onto the materials at a density of 5000 cells per well. GFP-HCECs were supplemented with keratinocyte serum-free medium (Gibco, Thermo Fisher Scientific, Waltham, MA, USA) containing bovine pituitary extract (0.05 mg/ml), epidermal growth factor (5 ng/ml), and penicillin/streptomycin (1 mg/ml), and their growth was monitored for 7 days in a humidified incubator at 37°C and 5% CO₂.

BMDC culture and flow cytometric analysis

With ethical permission from the Animal Care and Use Committee of Maisonneuve-Rosemont Hospital, bone marrow was isolated from the tibia and femur of male, C57BL/6J mice (6 to 12 weeks old) (36, 37). Cells were seeded on suspension culture plates with 1 × 10⁶ million cells per well in RPMI 1640 containing 10% (v/v) fetal bovine serum (FBS) (Wisent), penicillin-streptomycin-glutamine (0.5 mg/ml), 10 mM Hepes, 1 mM sodium pyruvate, 55 μm of β-mercaptoethanol, and granulocyte-macrophage colony-stimulating factor (25 ng/μl; GM-CSF) (all from Gibco, Thermo Fisher Scientific, Waltham, MA, USA). BMDCs were cultured for 6 days. RPMI-C containing GM-CSF (50 ng/ml) was exchanged for half of the media on days 2 and 3 of culture. On day 6, the cells were collected, and enlarged cells were selected using a Histodenz density gradient (Sigma-Aldrich, St. Louis, MO). The selected cells were seeded at a density of 1 × 10⁶ cells per well on a 24-well plate for materials testing.

For materials testing, BMDCs were incubated for 24 hours with a 6-mm, 500-μm-thick hydrogel disk. Individual hydrogel components CLP, PEG, CLP-PEG, DMTMM, fibrinogen, and thrombin were applied to the cells at a concentration equivalent to the hydrogel volume (table S1). LPS was used as a positive control for BMDC activation. BMDCs were labeled with direct-conjugate antibodies for CD11c, CD40, CD80, and CD86 (table S2) and Zombie Aqua Fixable Viability Kit (BioLegend, San Diego, CA). All samples were acquired using a BD LSR II and analyzed using FlowJo software (Becton, Dickinson and Company, Franklin Lakes, NJ, USA). BMDCs were selected using Zombie Aqua and CD11c as markers of a live, dendritic cell phenotype. Mean fluorescence for CD40, CD80, and CD86 was measured for the selected BMDCs and transformed into a ratio over the untreated BMDC control for analysis.

Macrophage polarization assay

Macrophages were isolated as previously described (38) with ethical permission from the Animal Care and Use Committee of the Ottawa

Heart Research Institute. Briefly, BMDMs were generated from the tibial bones of C57BL/6 female mice (8 to 10 weeks old). BMDMs were maintained for 1 week in DMEM with 10% FBS, 15% L929 media containing macrophage colony-stimulating factor and penicillin-streptomycin.

For the assay, BMDM precursors from female C57BL/6 mice (8 to 10 weeks old) were used. The wells of a 24-well culture plate were fitted with 18-mm circular glass coverslips. A portion of the coverslips was then coated with the LiQD Cornea. The hydrogel was allowed to set for 1 hour before it was washed three times with 1 ml of 1× PBS, followed by two additional 1-ml rinses with media before the seeding of cells. The BMDMs were seeded into the control wells and onto the material at a density of 200,000 cells per well. The plate was then placed in a humidified incubator at 37°C and 5% CO₂ with the media in each well being exchanged every 48 hours up to 7 days. On days 4 and 7, a subset of the wells was processed for immunofluorescence analysis to determine their polarization toward either an M1 or M2 phenotype. Briefly, media were removed, wells were washed two times with Hanks' buffer, and then, cells were fixed with a solution of 4% paraformaldehyde in 1× PBS at 4°C in the dark. Fixative was removed, and wells were washed two times with NH₄Cl in PBS, waiting 7 min between washes. The samples were then washed three times with 1× PBS. On the final wash, 0.2% NaN₃ was added from a 2% NaN₃ stock (10 μl/1 ml). When ready for staining, samples were washed with PBS and then blocked and permeabilized using a 2% bovine serum albumin in PBS solution containing 0.5% Triton X-100 for 1.5 hours at RT. Primary antibodies for CD206 and CD86 (table S1) were then diluted appropriately and added to the well plate to incubate overnight covered in foil at 4°C. The next day, wells were washed with 1× PBS. Secondary antibodies (table S1) were diluted and added to the plate and incubated at RT covered in foil for 1 hour. After 1 hour of incubation with the secondary antibodies, the wells were washed three times with 1× PBS. The coverslips were removed from the wells and mounted onto a glass slide using Prolong Gold antifade reagent with 4',6-diamidino-2-phenylindole (DAPI; Invitrogen, P36931). Cells were imaged with a Zeiss Axiovert 200M Fluorescence microscope equipped with an AxioCam MR camera using 63× oil immersion objective. The filters used were DAPI blue filter (excitation: 352 to 402/emission: 417 to 477), GFP green filter (excitation: 457 to 487/emission: 502 to 538), and Texas Red red filter (excitation: 542 to 582/emission: 604 to 644).

Rabbit perforation study

All experiments had ethical approval from the Western Sydney Local Health District Animal Ethics Committee. Three New Zealand white rabbits underwent controlled surgical perforation of the right eye under general anesthesia [sedation: medetomidine (25 mg/kg); analgesia: buprenorphine (0.5 mg/kg); anesthesia: ketamine (50 mg/kg), and 2% inhaled isoflurane]. A 3-mm surgical trephine was used to make a partial-thickness incision before full perforation using a 15° stab knife. The full incision was then enlarged to create a 1-mm full-thickness perforation. The perforation was filled with LiQD Cornea hydrogel and allowed to cross-link in situ. Air was injected into the anterior chamber to ensure that the perforation was completely sealed. For the 3 days after surgery, rabbits received 0.1% dexamethasone (Maxidex, Alcon Laboratories Pty Ltd, Australia) and 0.5% chloramphenicol eye drops (Chlorsig, Aspen Pharmacare, Australia) three times a day. Animals were monitored daily for signs of discomfort or glue leakage for the first week after surgery

and then twice weekly for subsequent weeks. Rabbits underwent follow-up clinical evaluation and slit lamp exams on days 1, 2, 3, 7, 14, 21, and 28 after surgery. At day 28 after surgery, rabbits were euthanized, and corneas from all operated and unoperated eyes were excised, fixed in 10% buffered formalin, and processed for paraffin embedding for histopathological examination (33).

In vivo study in Göttingen mini-pigs

In compliance with the Swedish Animal Welfare Ordinance and the Animal Welfare Act, and with ethical permission from the local ethical committee (Linköpings Djurförsöksetiska Nämnd), Göttingen mini-pigs underwent an anterior lamellar keratoplasty of the left eye. The left corneas were cut with a 6.5-mm surgical trephine to a depth of 500 μm , followed by blunt dissection of corneal stroma with a blade to create a wound bed. Four pigs received the LiQD Cornea formulation, which was cross-linked in situ and subsequently covered with human amniotic membrane that was secured with overlying sutures. Four pigs received syngeneic grafts, i.e., they were grafted with the tissue removed from another, albeit genetically coherent, pig in the group. Syngeneic grafts were secured with conventional interrupted sutures. The right contralateral corneas served as unoperated controls. After operation, the operated eyes received dexamethasone/tobramycin eye drops (Tobrasone, Alcon Laboratories, Sweden). Upon surgical completion, the pigs received a maintenance dose of one drop, three times per day for 5 days after surgery. Pigs were monitored daily for ocular health. Clinical exams were conducted under anesthesia before surgery and at 6 weeks, 3, 6, and 12 months after surgery. Clinical exams included slit lamp examination using a Kowa SL-15L portable slit lamp (Kowa Company Ltd., Aichi, Japan), anterior segment OCT (AS-OCT) to conduct corneal pachymetry (Optovue, Fremont, CA, USA), Schirmer's tear test (tear strips from TearFlo, Hub Pharmaceuticals, Rancho Cucamonga, CA, USA), esthesiometry to determine corneal sensitivity as a measure of nerve function (using a Cochet-Bonnet esthesiometer; Handaya Co., Tokyo, Japan), measurement of intraocular pressure (using a TonoVet tonometer, Icare Finland Oy, Vantaa, Finland), and in vivo confocal microscopy (Heidelberg HRT3 with a Rostock Cornea Module, Heidelberg Engineering GmbH, Dossenheim, Germany).

Central collagen content analysis

Central corneal biopsies (3 mm) were taken from each cornea and snap-frozen. For analyses, the samples were thawed and resuspended in 10 mM HCl at a ratio of 1:35 (w/v). Samples were digested using pepsin (1 mg/ml; Roche, Basel, Switzerland) at 2° to 8°C for 96 hours. The soluble fraction was recovered by centrifugation at 16,000g for 30 min at 2° to 4°C. An aliquot of the pepsin-soluble fraction was mixed with NuPAGE 4× LDS sample buffer (Life Technologies, Thermo Fisher Scientific, Waltham, MA, USA) denatured at 75°C for 8 min and analyzed on 3 to 8% tris-acetate gels under nonreducing conditions. Proteins were visualized by staining with Gelcode Blue (Pierce, Thermo Fisher Scientific, Waltham, MA, USA). Prestained broad-range marker (New England Biolabs, P7712) and porcine skin type I collagen (Koken Co. Ltd., Tokyo, Japan) were used as molecular weight standards. To quantitate the amounts of type I and type V collagens in control and operated corneas, densitometric scans of the stained gels were made to obtain relative numerical units using GE Healthcare ImageQuant 350 (GE Healthcare, Chicago, IL, USA).

Histopathology and immunohistochemistry

After removal of a central biopsy, a quarter of each operated and unoperated cornea was processed, paraffin-embedded, and stained with hematoxylin and eosin as described previously (32). Another quarter of each operated and unoperated cornea was treated with a sucrose gradient and fixed in 4% paraformaldehyde. The samples were frozen in optimal cutting temperature medium and sectioned at 8 or 10 μm before mounting on glass slides. Slides were washed in PBS before permeabilization in PBS with 0.3% Triton X-100 for 15 min. Slides were then washed in PBS. Sections stained using Alexa Fluor 488 or 647 secondary antibodies were incubated for 30 min in tris-buffered saline (TBS) containing 50 mM ammonium chloride to reduce background fluorescence. All sections were blocked for 1 hour at RT in PBS containing 5% normal goat serum or FBS with saponin (0.1 g/ml). Sections were stained with primary antibodies for cytokeratin 12, CD163, α -smooth muscle actin, and LYVE1 (table S3) overnight at 4°C in blocking solution. Slides were washed in PBS or TBS buffer containing 5% FBS and incubated with secondary antibodies (table S3) conjugated to Alexa Fluor 488 or 594 diluted at 1:1000 in blocking solution for 1 hour at RT. Sections stained using Alexa Fluor 488 or 647 secondary antibodies were quenched for autofluorescence using the Vector TrueVIEW Autofluorescence Quenching Kit (Vector Laboratories, Burlingame, CA, USA). Slides were stained with DAPI (5 $\mu\text{g}/\text{ml}$) for 10 min before mounting in Vectashield Antifade Mounting Medium or Vectashield Vibrance Mounting Medium (Vector Laboratories, Burlingame, CA, USA). Slides stained using lectin were washed in PBS, stained with lectin overnight at 4°C, washed, and counterstained with DAPI before mounting in Vectashield Antifade Mounting Medium. All slides were imaged using a Zeiss LSM 880 confocal microscope (Zeiss, Oberkochen, Germany). Two-dimensional images were processed using FIJI (39). EV and exosome staining using CD9 and Tsg101 was reconstructed as surfaces in Imaris v9.2.1 (Bitplane Inc., Concord, MA, USA) with an intensity threshold of 1.5 and 2 for CD9 and Tsg101, respectively, with a minimum voxel threshold of 10. A colocalization channel was built using the same intensity threshold as the surface reconstructions and converted into surfaces using a fluorescence intensity threshold of 0.5 and a minimum voxel threshold of 2.

Transmission electron microscopy

For TEM, a quarter of each cornea was fixed in 2.5% glutaraldehyde solution in 0.1 M sodium cacodylate buffer (pH 7.4). Samples were then cut in 1-mm-wide strips and postfixed in 1% OsO₄ solution for 2 hours. After dehydration in an ethanol gradient (50-70-90-95-100% ethanol), whole mounts were embedded in EMbed 812 (Electron Microscopy Sciences, Hatfield, Pennsylvania). Ultrathin sections were stained with lead citrate and examined using Tecnai G2 Spirit Bio Twin Microscope (FEI, Eindhoven, The Netherlands) at 120 kV.

Central cornea nerve analysis

In vivo confocal microscopy examinations were performed at various time points (before surgery and 3, 6, 9, and 12 months after surgery) throughout the 12-month mini-pig study. For each examination, all images with nerves were identified. For identification purposes, nerves were defined as bright, slender, straight, or branched structures; as substantially uniform in intensity along their length and width; and as having a marked contrast difference from the background

intensity level. Nerve tracing and analysis software NeuronJ) was used in combination with FIJI software to manually measure the total length of nerves present in each image identified as containing nerves (39). The central cornea nerve densities are reported from the average of the single-frame image displaying the highest nerve density for each treatment group and time point.

Evaluation of preliminary POC delivery system

Testing of the preliminary POC delivery system (fig. S3) was performed using the previously described ex vivo corneal perforation model. Briefly, a stock solution consisting of 10% CLP-PEG and 1% fibrinogen was heated to 50°C and transferred to a 1-ml disposable BD syringe. An equal volume of 10% (w/w) DMTMM in 10 mM PBS was added to a second 1-ml disposable BD syringe. The syringes were then attached to a dual-syringe adapter (Medmix Systems AG, Switzerland), which was fitted with a 1:1 static mixer (Medmix Systems AG, Switzerland) and a 19 gauge-by-25 mm flattened tip cannula. The mixing system was heated to 50°C, and the material was dispensed through the mixing system into the wound bed to which a solution of thrombin (250 U/ml) had been applied.

Statistical analyses

The in vitro statistical analysis for BMDCs was performed using an unpaired, two-way *t* test with a confidence interval of 95% for each marker (GraphPad Prism 8.3.0, GraphPad Software LLC., San Diego, CA, USA). The unit of analysis was the mouse ($n = 6$ per group). The unit of analysis for the clinical statistics was the eye. The clinical statistics were conducted on uneven population sizes (LiQD Cornea: $n = 4$; syngeneic graft: $n = 4$; unoperated: $n = 8$). For variables with repeated measures over time, a mixed-effects analysis with Geisser-Greenhouse's correction was performed ($\alpha = 0.05$) with Tukey's multiple comparisons test for treatment effects by time point (GraphPad Prism 8.3.0). Postmortem collagen content analysis was performed using a one-way analysis of variance (ANOVA) for each collagen type with a Tukey post hoc test ($\alpha = 0.05$) (IBM SPSS Statistics version 25, IBM Corp., Armonk, NY, USA). All graphs were prepared using GraphPad Prism, and data are displayed as mean with individual data points or mean \pm SEM.

SUPPLEMENTARY MATERIALS

Supplementary material for this article is available at <http://advances.sciencemag.org/cgi/content/full/6/25/eaba2187/DC1>

REFERENCES AND NOTES

- M. S. Oliva, T. Schottman, M. Gulati, Turning the tide of corneal blindness. *Indian J. Ophthalmol.* **60**, 423–427 (2012).
- P. Gain, R. Jullienne, Z. He, M. Aldossary, S. Acquart, F. Cognasse, G. Thuret, Global survey of corneal transplantation and eye banking. *JAMA Ophthalmol.* **134**, 167–173 (2016).
- V. Jhanji, A. L. Young, J. S. Mehta, N. Sharma, T. Agarwal, R. B. Vajpayee, Management of corneal perforation. *Surv. Ophthalmol.* **56**, 522–538 (2011).
- P. Jarrett, A. Coury, Tissue adhesives and sealants for surgical applications. In *Joining and Assembly of Medical Materials and Devices*, Y. Zhou, M. D. Breyen, Eds. (Woodhead Publishing, 2013), pp. 449–490.
- B. J. Vote, M. J. Elder, Cyanoacrylate glue for corneal perforations: A description of a surgical technique and a review of the literature. *Clin. Exp. Ophthalmol.* **28**, 437–442 (2000).
- H. Yokogawa, A. Kobayashi, N. Yamazaki, T. Masaki, K. Sugiyama, Surgical therapies for corneal perforations: 10 years of cases in a tertiary referral hospital. *Clin. Ophthalmol.* **8**, 2165–2170 (2014).
- M. Vanathi, N. Sharma, J. S. Titiyal, R. Tandon, R. B. Vajpayee, Tectonic grafts for corneal thinning and perforations. *Cornea* **21**, 792–797 (2002).

- A. Khodadoust, A. P. Quinter, Microsurgical approach to the conjunctival flap. *Arch. Ophthalmol.* **121**, 1189–1193 (2003).
- K. Hanada, J. Shimazaki, S. Shimamura, K. Tsubota, Multilayered amniotic membrane transplantation for severe ulceration of the cornea and sclera. *Am. J. Ophthalmol.* **131**, 324–331 (2001).
- C. E. Hugkustone, Use of a bandage contact lens in perforating injuries of the cornea. *J. R. Soc. Med.* **85**, 322–323 (1992).
- E. Shirzaei Sani, A. Kheirkhah, D. Rana, Z. Sun, W. Foulsham, A. Sheikh, A. Khademhosseini, R. Dana, N. Annabi, Sutureless repair of corneal injuries using naturally derived bioadhesive hydrogels. *Sci. Adv.* **5**, eaav1281 (2019).
- S. Guhan, S. L. Peng, H. Janbatian, S. Saadeh, S. Greenstein, F. Al Bahrani, A. Fadlallah, T. C. Yeh, S. A. Melki, Surgical adhesives in ophthalmology: History and current trends. *Br. J. Ophthalmol.* **102**, 1328–1335 (2018).
- A. Sharma, R. Kaur, S. Kumar, P. Gupta, S. Pandav, B. Patnaik, A. Gupta, Fibrin glue versus *N*-butyl-2-cyanoacrylate in corneal perforations. *Ophthalmology* **110**, 291–298 (2003).
- S. Hoshi, F. Okamoto, M. Arai, T. Hirose, Y. Sugiura, Y. Kaji, T. Oshika, In vivo and in vitro feasibility studies of intraocular use of polyethylene glycol-based synthetic sealant to close retinal breaks in porcine and rabbit eyes. *Invest. Ophthalmol. Vis. Sci.* **56**, 4705–4711 (2015).
- T. Nakayama, C. Aizawa, Change in gelatin content of vaccines associated with reduction in reports of allergic reactions. *J. Allergy Clin. Immunol.* **106**, 591–592 (2000).
- G. Wollensak, E. Spörl, F. Reber, L. Pillunat, R. Funk, Corneal endothelial cytotoxicity of riboflavin/UVA treatment in vitro. *Ophthalmic Res.* **35**, 324–328 (2003).
- L. Koivusalo, M. Kauppila, S. Samanta, V. S. Parihar, T. Ilmarinen, S. Miettinen, O. P. Oommen, H. Skottman, Tissue adhesive hyaluronic acid hydrogels for sutureless stem cell delivery and regeneration of corneal epithelium and stroma. *Biomaterials* **225**, 119516 (2019).
- P. Fagerholm, N. S. Lagali, K. Merrett, W. B. Jackson, R. Munger, Y. Liu, J. W. Polarek, M. Söderqvist, M. Griffith, A biosynthetic alternative to human donor tissue for inducing corneal regeneration: 24-month follow-up of a phase 1 clinical study. *Sci. Transl. Med.* **2**, 46ra61 (2010).
- P. Fagerholm, N. S. Lagali, J. A. Ong, K. Merrett, W. B. Jackson, J. W. Polarek, E. J. Suuronen, Y. Liu, I. Brunette, M. Griffith, Stable corneal regeneration four years after implantation of a cell-free recombinant human collagen scaffold. *Biomaterials* **35**, 2420–2427 (2014).
- J. R. Jangamreddy, M. K. C. Haagdorens, M. Mirazul Islam, P. Lewis, A. Samanta, P. Fagerholm, A. Liszka, M. K. Ljunggren, O. Buznyk, E. I. Alarcon, N. Zakaria, K. M. Meek, M. Griffith, Short peptide analogs as alternatives to collagen in pro-regenerative corneal implants. *Acta Biomater.* **69**, 120–130 (2018).
- R. J. Mullins, C. Richards, T. Walker, Allergic reactions to oral, surgical and topical bovine collagen: Anaphylactic risk for surgeons. *Aust. N. Z. J. Ophthalmol.* **24**, 257–260 (1996).
- J. A. Fishman, Infectious disease risks in xenotransplantation. *Am. J. Transplant.* **18**, 1857–1864 (2018).
- C. Samarawickrama, A. Samanta, A. Liszka, P. Fagerholm, O. Buznyk, M. Griffith, B. Allan, Collagen-based fillers as alternatives to cyanoacrylate glue for the sealing of large corneal perforations. *Cornea* **37**, 609–616 (2018).
- K. Araki-Sasaki, Y. Ohashi, T. Sasabe, K. Hayashi, H. Watanabe, Y. Tano, H. Handa, An SV40-immortalized human corneal epithelial cell line and its characterization. *Invest. Ophthalmol. Vis. Sci.* **36**, 614–621 (1995).
- Y. Qazi, P. Hamrah, Corneal allograft rejection: Immunopathogenesis to therapeutics. *J. Clin. Cell Immunol.* **2013**, 006 (2013).
- H. Simianer, F. Köhn, Genetic management of the Göttingen minipig population. *J. Pharmacol. Toxicol. Methods* **62**, 221–226 (2010).
- I. Ahmed, Z. Akram, H. M. N. Iqbal, A. L. Munn, The regulation of endosomal sorting complex required for transport and accessory proteins in multivesicular body sorting and enveloped viral budding - An overview. *Int. J. Biol. Macromol.* **127**, 1–11 (2019).
- C. Théry, K. W. Witwer, E. Aikawa, M. J. Alcaraz, J. D. Anderson, R. Andriantsitohaina, A. Antoniou, T. Arab, F. Archer, G. K. Atkin-Smith, D. C. Ayre, J.-M. Bach, D. Bachurski, H. Baharvand, L. Balaj, S. Baldacchino, N. N. Bauer, A. A. Baxter, M. Bewaby, C. Beckham, A. Bedina Zavec, A. Benmoussa, A. C. Berardi, P. Bergese, E. Bielska, C. Blenkinson, S. Bobis-Wozowicz, E. Boilard, W. Boireau, A. Bongiovanni, F. E. Borràs, S. Bosch, C. M. Boulanger, X. Breakefield, A. M. Breglio, M. A. Brennan, D. R. Brigstock, A. Brisson, M. L. D. Broekman, J. F. Bromberg, P. Bryl-Górecka, S. Buch, A. H. Buck, D. Burger, S. Busatto, D. Buschmann, B. Bussolati, E. I. Buzás, J. B. Byrd, G. Camussi, D. R. F. Carter, S. Caruso, L. W. Chamley, Y.-T. Chang, C. Chen, S. Chen, L. Cheng, A. R. Chin, A. Clayton, S. P. Clerici, A. Cocks, E. Cocucci, R. J. Coffey, A. Cordeiro-da-Silva, Y. Couch, F. A. Coumans, B. Coyle, R. Crescitelli, M. F. Criado, C. D'Souza-Schorey, S. Das, A. Datta Chaudhuri, P. de Candia, E. F. De Santana, O. De Wever, H. A. del Portillo, T. Demaret, S. Deville, A. Devitt, B. Dhondt, D. Di Vizio, L. C. Dieterich, V. Dolo, A. P. Dominguez Rubio, M. Dominici, M. R. Dourado, T. A. P. Driedonks, F. V. Duarte, H. M. Duncan, R. M. Eichenberger, K. Ekström, S. El Andaloussi, C. Elie-Caille, U. Erdbrügger, J. M. Falcón-Pérez, F. Fatima, J. E. Fish, M. Flores-Bellver, A. Försönits, A. Fretlet-Barrand, F. Fricke, G. Fuhrmann, S. Gabrielsson, A. Gámez-Valero, C. Gardiner, K. Gärtner, R. Gaudin,

- Y. S. Gho, B. Giebel, C. Gilbert, M. Gimona, I. Giusti, D. C. I. Goberdhan, A. Örgens, S. M. Gorski, D. W. Greening, J. C. Gross, A. Gualerzi, G. N. Gupta, D. Gustafson, A. Handberg, R. A. Haraszti, P. Harrison, H. Hegyesi, A. Hendrix, A. F. Hill, F. H. Hochberg, K. F. Hoffmann, B. Holder, H. Holthofer, B. Hosseinkhani, G. Hu, Y. Huang, V. Huber, S. Hunt, A. G.-E. Ibrahim, T. Ikezu, J. M. Inal, M. Isin, A. Ivanova, H. K. Jackson, S. Jacobsen, S. M. Jay, M. Jayachandran, G. Jenster, L. Jiang, S. M. Johnson, J. C. Jones, A. Jong, T. Jovanovic-Talisman, S. Jung, R. Kalluri, S. Kano, S. Kaur, Y. Kawamura, E. T. Keller, D. Khamari, E. Khomyakova, A. Khorova, P. Kierulf, K. P. Kim, T. Kislinger, M. Klingeborn, D. J. Klinke, M. Kornek, M. M. Kosanović, Á. F. Kovács, E.-M. Krämer-Albers, S. Krasemann, M. Krause, I. V. Kurochkin, G. D. Kusuma, S. Kuypers, S. Laitinen, S. M. Langevin, L. R. Languino, J. Lannigan, C. Lässer, L. C. Laurent, G. Lavieu, E. Lázaro-Ibáñez, S. Le Lay, M.-S. Lee, Y. X. F. Lee, D. S. Lemos, M. Lenassi, A. Leszczynska, I. T. S. Li, K. Liao, S. F. Libregts, E. Ligeti, R. Lim, S. K. Lim, A. Linč, K. Linnemannstons, A. Lorente, C. A. Lombard, M. J. Lorenowicz, Á. M. Lörcz, J. Lötvall, J. Lovett, M. C. Lowry, X. Loyer, Q. Lu, B. Lukomska, T. R. Lunavat, S. L. N. Maas, H. Malhi, A. Marcilla, J. Mariani, J. Mariscal, E. S. Martens-Uzunova, L. Martin-Jaular, M. C. Martinez, V. R. Martins, M. Mathieu, S. Mathivanan, M. Mauger, L. K. McGinnis, M. J. McVey, D. G. Meckes, K. L. Meehan, I. Mertens, V. R. Minciacci, A. Möller, M. M. Jørgensen, A. Morales-Kastresana, J. Morhayim, F. Mullier, M. Muraca, L. Musante, V. Mussack, D. C. Muth, K. H. Myburgh, T. Najrana, M. Nawaz, I. Nazarenko, P. Nejsun, C. Neri, T. Neri, R. Nieuwland, L. Nimrichter, J. P. Nolan, E. N. Nolte-’t Hoen, N. Noren Hooten, L. O’Driscoll, T. O’Grady, A. O’Loghlen, T. Ochiai, M. Olivier, A. Ortiz, L. A. Ortiz, X. Osteikoetxea, O. Østergaard, M. Ostrowski, J. Park, D. M. Pegtel, H. Peinado, F. Perut, M. W. Pfaffi, D. G. Phinney, B. C. H. Pieters, R. C. Pink, D. S. Pisetsky, E. Pogge von Strandmann, I. Polakovicova, I. K. H. Poon, B. H. Powell, I. Prada, L. Pulliam, P. Quesenberry, A. Radeghieri, R. L. Raffai, S. Raimondo, J. Rak, M. I. Ramirez, G. Raposo, M. S. Rayyan, N. Regev-Rudzi, F. L. Ricklefs, P. D. Robbins, D. D. Roberts, S. C. Rodrigues, E. Rohde, S. Rome, K. M. A. Rouschop, A. Rugghetti, A. E. Russell, P. Saá, S. Sahoo, E. Salas-Huenuleo, C. Sánchez, J. A. Saugstad, M. J. Saul, R. M. Schiffellers, R. Schneider, T. H. Schøyen, A. Scott, E. Shahaj, S. Sharma, O. Shatnyeva, F. Shekari, G. V. Shelke, A. K. Shetty, K. Shiba, P. R. M. Siljander, A. M. Silva, A. Skowronek, O. L. Snyder, R. P. Soares, B. W. Sódar, C. Soekmadji, J. Sotillo, P. D. Stahl, W. Stoorvogel, S. L. Stott, E. F. Strasser, S. Swift, H. Tahara, M. Tewari, K. Timms, S. Tiwari, R. Tixeira, M. Tkach, W. S. Toh, R. Tomasini, A. C. Torrecilhas, J. P. Tosar, V. Toxavidis, L. Urbanelli, P. Vader, B. W. M. van Balkom, S. G. van der Grein, J. Van Deun, M. J. C. van Herwijnen, K. Van Keuren-Jensen, G. van Niel, M. E. van Royen, A. J. van Wijnen, M. H. Vasconcelos, I. J. Vechetti, T. D. Veit, L. J. Vella, É. Velot, F. J. Verweij, B. Vestad, J. L. Viñas, T. Visnovitz, K. V. Vukman, J. Wahlgren, D. C. Watson, M. H. M. Wauben, A. Weaver, J. P. Webber, V. Weber, A. M. Wehman, D. J. Weiss, J. A. Welsh, S. Wendt, A. M. Wheelock, Z. Wiener, L. Witte, J. Wolfram, A. Xagorari, P. Xander, J. Xu, X. Yan, M. Yáñez-Mó, H. Yin, Y. Yuan, V. Zappulli, J. Zarubova, V. Žekas, J. Y. Zhang, Z. Zhao, L. Zheng, A. R. Zheutlin, A. M. Zickler, P. Zimmermann, A. M. Zivkovic, D. Zocco, E. K. Zuba-Surma, Minimal information for studies of extracellular vesicles 2018 (MISEV2018): A position statement of the international society for extracellular vesicles and update of the MISEV2014 guidelines. *J. Extracell. Vesicles* **7**, 1535750 (2018).
29. R. J. Barry, A. K. Denniston, *A Dictionary of Ophthalmology* (Oxford Univ. Press, 2017).
30. Y. Sano, B. R. Ksander, J. W. Streilein, Minor H, rather than MHC, alloantigens offer the greater barrier to successful orthotopic corneal transplantation in mice. *Transpl. Immunol.* **4**, 53–56 (1996).
31. M. M. Alvarez, J. C. Liu, G. Trujillo-de Santiago, B.-H. Cha, A. Vishwakarma, A. M. Ghaemmaghami, A. Khademhosseini, Delivery strategies to control inflammatory response: Modulating M1-M2 polarization in tissue engineering applications. *J. Control. Release* **240**, 349–363 (2016).
32. M. K. Ljunggren, R. A. Elizondo, E. Edin, D. Olsen, K. Merrett, C.-J. Lee, G. Salerud, J. Polarek, P. Fagerholm, M. Griffith, Effect of surgical technique on corneal implant performance. *Transl. Vis. Sci. Technol.* **3**, 6 (2014).
33. Y. Liu, L. Gan, D. J. Carlsson, P. Fagerholm, N. Lagali, M. A. Watsky, R. Munger, W. G. Hodge, D. Priest, M. Griffith, A simple, cross-linked collagen tissue substitute for corneal implantation. *Invest. Ophthalmol. Vis. Sci.* **47**, 1869–1875 (2006).
34. K. A. Williams, M. C. Keane, N. E. Coffey, V. J. Jones, R. A. D. Mills, D. J. Coster, *The Australian Corneal Graft Registry* (Flinders Univ., 2018).
35. M. M. Islam, R. Ravichandran, D. Olsen, M. K. Ljunggren, P. Fagerholm, C. J. Lee, M. Griffith, J. Phopase, Self-assembled collagen-like-peptide implants as alternatives to human donor corneal transplantation. *RSC Adv.* **6**, 55745–55749 (2016).
36. Y. I. Son, S. Egawa, T. Tatsumi, R. E. Redlinger Jr., P. Kalinski, T. Kanto, A novel bulk-culture method for generating mature dendritic cells from mouse bone marrow cells. *J. Immunol. Methods* **262**, 145–157 (2002).
37. K. Inaba, M. Inaba, N. Romani, H. Aya, M. Deguchi, S. Ikehara, S. Muramatsu, R. M. Steinman, Generation of large numbers of dendritic cells from mouse bone marrow cultures supplemented with granulocyte/macrophage colony-stimulating factor. *J. Exp. Med.* **176**, 1693–1702 (1992).
38. J. Weischenfeldt, B. Porse, Bone marrow-derived macrophages (BMM): Isolation and applications. *CSH Protoc.* **2008**, pdb.prot5080 (2008).
39. J. Schindelin, I. Arganda-Carreras, E. Frise, V. Kaynig, M. Longair, T. Pietzsch, S. Preibisch, C. Rueden, S. Saalfeld, B. Schmid, J.-Y. Tinevez, D. J. White, V. Hartenstein, K. Eliceiri, P. Tomancak, A. Cardona, Fiji: An open-source platform for biological-image analysis. *Nat. Methods* **9**, 676–682 (2012).

Acknowledgments: We thank S. Lesage and C. Audiger for help with the dendritic cell assay design and J. Laganieri and B. Hosseinpour for assistance with histopathological processing.

Funding: We acknowledge research funding from the Euronanomed II–Swedish Research Council (Dnr IKE-2014-00597), the Euronanomed III–FRQS (file no. 278653), and the Quebec Vision Health Research Network–FRQS (file no. 2017-3). C.D.M. was supported by a Caroline Durand Foundation Research Chair for Cellular Therapy in the Eye to M. Griffith. B.D.A. receives partial salary support for research from the NIHR Biomedical Research Centre (BRC-1215-20002) at the Moorfields Eye Hospital NHS Foundation Trust and the UCL Institute of Ophthalmology. C.S. acknowledges support from a Westmead Charitable Trust Early Career Research Fellowship (CC368629-8245), and F.C.S. acknowledges support for her doctoral studies from the Faculté des études supérieures et postdoctorales de l’Université de Montréal, Fonds de recherche en ophtalmologie de l’Université de Montréal (FROUM), Fonds de recherche du Québec-Nature et technologies (FRQNT), and the Natural Sciences and Engineering Research Council of Canada (NSERC). **Author contributions:** B.D.A. and M. Griffith developed the LiQD Cornea concept. C.D.M. and M. Griffith designed the material. C.D.M. performed all optical, physical, mechanical, and chemical characterization and BMDM assays and assisted with animal surgeries and analyses of the results. F.C.S. performed the dendritic assays, immunohistochemistry, and analyses of the clinical results from the pig study. B.D.A. and C.S. designed the LiQD Corneal animal studies for feasibility evaluation. C.S. and D.H. performed the rabbit perforation study. O.B. and P.F. performed the pig surgeries and follow-ups. M.H. and M.K.L. contributed to the pig study design and assisted with pig clinical exams. D.O. conducted the collagen content analysis. M.H., I.P., and P.L. contributed to the transmission electron microscopy and interpretation of the results. M. Groleau contributed to the immunohistochemistry experiments. E.E. contributed in IHC protocol development and statistical analysis. M. Griffith developed the overall study plan and supervised all research and analyses. All authors contributed to the writing, revisions, and final approval of the manuscript. **Competing interests:** M. Griffith is a named inventor on PCT PCT/IB2017/056342 Collagen and CLP-based hydrogels, corneal implants, filler glue, and uses thereof, which was assigned to the Hyderabad Eye Research Foundation, and then subsequently assigned to North Grove Investments Inc. wherein PCT national phase applications have been filed in the United States, Europe, India, China, and Canada. C.D.M. and M. Griffith are named inventors on a U.S. provisional patent application no. 62916765, subsequent to a disclosure to Univalor, technology transfer agent to Maisonneuve-Rosemont Hospital and Université de Montréal. The authors declare that they have no other competing interests. **Data and materials availability:** All data needed to evaluate the conclusions in the paper are present in the paper and/or the Supplementary Materials. Additional data related to this paper may be requested from the authors.

Submitted 14 November 2019

Accepted 8 May 2020

Published 17 June 2020

10.1126/sciadv.aba2187

Citation: C. D. McTiernan, F. C. Simpson, M. Haagdoorens, C. Samarawickrama, D. Hunter, O. Buznyk, P. Fagerholm, M. K. Ljunggren, P. Lewis, I. Pintelon, D. Olsen, E. Edin, M. Groleau, B. D. Allan, M. Griffith, LiQD Cornea: Pro-regeneration collagen mimetics as patches and alternatives to corneal transplantation. *Sci. Adv.* **6**, eaba2187 (2020).

LiQD Cornea: Pro-regeneration collagen mimetics as patches and alternatives to corneal transplantation

Christopher D. McTiernan, Fiona C. Simpson, Michel Haagdorens, Chameen Samarawickrama, Damien Hunter, Oleksiy Buznyk, Per Fagerholm, Monika K. Ljunggren, Philip Lewis, Isabel Pintelon, David Olsen, Elle Edin, Marc Groleau, Bruce D. Allan and May Griffith

Sci Adv 6 (25), eaba2187.
DOI: 10.1126/sciadv.aba2187

ARTICLE TOOLS

<http://advances.sciencemag.org/content/6/25/eaba2187>

SUPPLEMENTARY MATERIALS

<http://advances.sciencemag.org/content/suppl/2020/06/15/6.25.eaba2187.DC1>

REFERENCES

This article cites 36 articles, 7 of which you can access for free
<http://advances.sciencemag.org/content/6/25/eaba2187#BIBL>

PERMISSIONS

<http://www.sciencemag.org/help/reprints-and-permissions>

Use of this article is subject to the [Terms of Service](#)

Science Advances (ISSN 2375-2548) is published by the American Association for the Advancement of Science, 1200 New York Avenue NW, Washington, DC 20005. The title *Science Advances* is a registered trademark of AAAS.

Copyright © 2020 The Authors, some rights reserved; exclusive licensee American Association for the Advancement of Science. No claim to original U.S. Government Works. Distributed under a Creative Commons Attribution NonCommercial License 4.0 (CC BY-NC).